

Phytoplankton regulation in a eutrophic tidal river (San Joaquin River, California)

Alan D. Jassby¹

July 12, 2004

This manuscript has been tentatively accepted for publication in San Francisco Estuary and Watershed Science, but has not yet been revised in response to reviewer comments. Please wait for final version before citing.

AJ
9/29/04

¹Department of Environmental Science and Policy, University of California, Davis, CA 95616 USA (adjassby@ucdavis.edu)

Abstract

As in many U.S. estuaries, the tidal San Joaquin River exhibits elevated organic matter production that interferes with beneficial use of the river for drinking water, habitat, and fish spawning and migration. High phytoplankton biomass in the tidal river is, accordingly, a focus of management strategies. An unusually long and comprehensive monitoring dataset enabled us to identify the determinants of phytoplankton concentration. Phytoplankton carrying capacity may be set by nitrogen or phosphorus during extreme drought years. But in most years, growth rate is light-limited and phytoplankton concentration depends primarily on river discharge, which determines the cumulative light exposure in transit downstream. The concentration-discharge relationship has shifted over the years, for reasons as yet unknown. Only very large decreases in nonpoint nutrient sources would limit phytoplankton concentration reliably. Growth rate and concentration could increase if nonpoint source management decreases mineral suspended load but does not decrease nutrient load sufficiently. Small changes in water storage and release patterns due to dam operation have a profound influence on peak phytoplankton concentration, and offer a near-term approach for management of blooms. Water exports from the tidal San Joaquin River also affect residence time during passage downstream and may have resulted in more than a doubling of peak concentration in some years.

keywords anthropogenic effects, climate and interannual variability, dams, estuary, light, nutrients and nutrient cycling, plankton, rivers, runoff and streamflow, turbidity

Contents

1	Introduction	2
1.1	Study Area	4
2	Methods	5
2.1	Data Sources	5
2.2	Phytoplankton and Optical Parameters	6
2.3	Hydrological Estimates	10
2.4	Data Analysis	11
3	Results	13
3.1	Historical Time Series	13
3.2	Resource Constraints on Carrying Capacity and Growth Rates	14
3.3	Phytoplankton Biomass and River Discharge	17
3.4	Net River Discharge and Export Effects	19
4	Discussion	21
4.1	Nutrient Management and Phytoplankton	21
4.2	Light-Attenuating Materials	23
4.3	River Discharge	24
4.4	Concluding Remarks	27
5	Acknowledgments	29
6	References	29
7	Tables	34
8	Figure Captions	34

1 Introduction

Most estuaries in the U.S. exhibit moderate to high eutrophic conditions and elevated macronutrient concentrations (Bricker et al. 1999). Increased organic matter production and depleted dissolved oxygen are common symptoms, resulting in habitat loss, fish kills, and sometimes offensive odors. The tidal San Joaquin River, one of two major rivers draining into the San Francisco Estuary, is a representative of this general pattern. Phytoplankton chlorophyll *a* concentrations sometimes exceed 300 $\mu\text{g/L}$ in summer, leading to several deleterious consequences. Water is diverted from the tidal river for export via state and federal water conveyances to millions of Californians for drinking water. The high total organic carbon content of this water, due in part to phytoplankton organic matter, enhances the production of harmful disinfection by-products such as trihalomethanes when disinfectants such as chlorine are added to drinking water to kill microbial pathogens (Lam et al. 1994). Further downstream, the river frequently exhibits low dissolved oxygen conditions and annually violates regional water quality objectives. This chronic hypoxia interferes with several beneficial uses of the river, including spawning and migration of warm (striped bass, sturgeon, and shad) and cold (salmon and steelhead) freshwater fishes, as well as warm and cold freshwater species habitat (CVRWQCB 1998, 2003). Phytoplankton biomass transported from upstream of low dissolved oxygen locations is considered to be a major source of oxygen-demanding materials and has been targeted for management.

Most estuaries showing high levels of eutrophic conditions are also moderately to highly influenced by human-related nutrient inputs (e.g., wastewater treatment and agriculture), which have therefore been identified as the most important management targets on a national basis. It is natural to assume that such a course is merited for the San Joaquin River as well, especially because of the intensity of agriculture and animal husbandry throughout the watershed, resulting in nonpoint sources extending along the river within and upstream of the estuary. However, many uncertainties surround the regulation of phytoplankton concentrations in tidal rivers. Regional differences in nutrient sources and estuarine functioning are significant. Nutrient limitation appears to be generally lacking in large rivers (Wehr and Descy 1998), but there are many exceptions. Basu and

Pick (1996), for example, found no relation between chlorophyll *a* and residence time in 31 rivers of eastern Canada. Rather, determination by macronutrients was much more common. Billen et al. (1994), using a simulation of the Seine River system, demonstrated how hydrological factors determine the time of onset and the position within the drainage network of the spring algal bloom, but it is phosphorus that determines the size. More generally, Cloern (2001) has emphasized the spectrum of estuarine responses to increased nutrient loading—from resistant to highly sensitive. He showed that a variety of attributes can act as a filter to modify effects of excessive nutrients, including the strength of tidal mixing, magnitude of horizontal transport, optical water quality, and abundance of benthic suspension-feeders. The early conceptual model linking nutrient loading inexorably to biomass accumulation, derived largely from experience with lakes, is now understood to be inadequate for understanding estuarine systems, including their tidal river reaches.

We need to ask, then, what controls phytoplankton biomass in the tidal San Joaquin River upstream of major water export diversions and low dissolved oxygen conditions, how will reduction in nutrient loading affect existing phytoplankton levels, and what other opportunities exist to manage phytoplankton in this river reach? Strategies for phytoplankton regulation in this subregion of the estuary must also consider the negative consequences of *low* phytoplankton biomass. The tidal river is one of the few productive habitats for an estuarine food web that otherwise appears to be unproductive and food-limited (Sobczak et al. 2002), and the small centric diatoms that dominate the reach are a highly nutritious base for the food web supporting higher organisms. The goal, then, should not be to aim for arbitrarily low levels, but rather to explore ways in which phytoplankton biomass can be regulated more finely, if possible.

One relevant resource that has not been utilized is the large collection of retrospective data for the upper estuary. Several government agencies have maintained monitoring programs for decades, mostly for determining compliance with water quality objectives. This dataset—the result of a sustained commitment to environmental monitoring by the California departments of Water Resources and Fish and Game and the U.S. Bureau of Reclamation—is exceptional in its spatial coverage, its duration, and its multiplicity of measured variables. It has proven useful for analysis

of long-term trends and interannual variability in primary productivity, phytoplankton biomass, and phytoplankton community composition (Lehman 2000, Jassby et al. 2002) in various subregions of the Delta. Particularly important for the San Francisco Estuary is an analysis that encompasses drought and flood years. Interannual variability in freshwater flow to this estuary is high, and the biota show one of the strongest and broadest responses to flow among large estuaries (Kimmerer 2002). Conclusions from a single year or too small a subset of climatic conditions are bound to be misleading. Because the programs were not designed to answer many of the questions that have arisen in relation to the hypoxia problem, there are relative inadequacies in the data set, including absence of certain water quality variables, low temporal resolution, and data gaps. Nonetheless, the data, which span climate extremes, present an opportunity to investigate the issues from a new and informative perspective, namely, in the context of long-term behavior of the system. Here, the Delta dataset is used to determine the regulating factors for river phytoplankton biomass in a eutrophied tidal river and, more specifically, to close further the gap in understanding for the lower San Joaquin River. The analysis also highlights some difficult implications for managing phytoplankton organic matter loads in turbid eutrophic systems.

1.1 Study Area

The tidal San Joaquin River is located in the upper part of the estuary known as the Delta, a mosaic of waterways linking the great rivers of northern California to the downstream embayments comprising San Francisco Bay; together, the Delta and Bay form the San Francisco Estuary. The San Joaquin River extends from the westernmost Delta upstream past the city of Fresno, draining a watershed area of about 19,000 km² (Kratzer et al. 2004; Figure 1). Its river valley is a major center of agricultural production. Despite the loss of most of its wetlands, it also remains a critical habitat for fish and wildlife, including many federally listed threatened and endangered plants and animals. Hydrology of the river and its major tributaries—the Merced, Tuolumne, and Stanislaus rivers—upstream of the Delta is highly managed through dams, diversions, and artificial conveyances. The river reaches the southern boundary of the Delta near the town of Vernalis, where estuarine tides

begin to affect its flow (Figure 2). The long-term (1956–2002) mean flow at this point is about $130 \text{ m}^3 \text{ s}^{-1}$, with annual means ranging from $13 \text{ m}^3 \text{ s}^{-1}$ in 1961 to $650 \text{ m}^3 \text{ s}^{-1}$ in 1983 (IEP 2003). Past Mossdale, a portion of the water is diverted down Old River to Clifton Court Forebay, where it is exported for agricultural, industrial, and domestic use, including drinking water for 22 million state residents, through large pumping facilities feeding the State Water Project (California Aqueduct) and federal Central Valley Project (Delta–Mendota Canal). Annually, temporary barriers have been placed at the head of Old River to increase flows down the mainstem, with the intention of alleviating low dissolved oxygen conditions downstream and facilitating fish migration. Water is also diverted for irrigation in the Delta by numerous siphons; much of this water is lost to evapotranspiration, although some returns through many agricultural drainage points. The river is about 2.5–3.5 m deep and 50 m wide between Vernalis station and the Stockton Deep Water Ship Channel (Ship Channel), a portion of the river between San Francisco Bay and the city that has been dredged to allow the passage of ocean-going vessels to the city’s port. Just upstream of the Ship Channel, the Regional Wastewater Control Facility (RWCF) discharges its effluent into the river. The river enters the Ship Channel at the eastern point of Rough and Ready Island. River width increases to about 75 m in the Ship Channel, and it is dredged to a depth of 11 m between the Port of Stockton and the Bay. The tidal range is about 1 m in this region. Low dissolved oxygen conditions occur in the Ship Channel from approximately the Turning Basin at the Port of Stockton downstream to Turner Cut.

2 Methods

2.1 Data Sources

A variety of data sources were used in this study. Of particular note is the discrete water quality monitoring program, which collects data from throughout the Delta on a monthly basis, approximately. The number of baseline monitoring stations has ranged from a high of 26 to the current 11 stations. The program was originally started by the U.S. Bureau of Reclamation in

the late 1960s. It is now carried out jointly with the California Department of Water Resources, assisted by the California Department of Fish and Game and the U.S. Geological Survey, under the auspices of the Interagency Ecological Program's Environmental Monitoring Program (EMP). Its primary purpose is to provide information for compliance with flow-related water quality standards specified in water rights permits that allow export by the state and federal water projects. This data set, unusual in its spatial and temporal coverage, as well as the variety of variables considered, is the main evidence used in this report for water quality of the San Joaquin River upstream of the Ship Channel. The two stations relevant to this study are the Vernalis and Mossdale stations (Figure 2) on the tidal river upstream of the Ship Channel. Water quality variables utilized here include chlorophyll *a*, phytoplankton taxa, total suspended solids and turbidity, vertical light attenuation coefficient, total nitrogen and phosphorus, silica, and temperature. A detailed description of the sampling and analytical methods can be accessed at http://www.iep.ca.gov/emp/Metadata/metadata_index.html. The longest record for phytoplankton concentration in terms of chlorophyll *a* is at Vernalis, where it has been measured regularly since 1969. The time series for Mossdale began only in 1975 and was interrupted in 1995. We therefore focused on Vernalis, using Mossdale data when necessary for certain calculations. Within each series, the gaps are few.

2.2 Phytoplankton and Optical Parameters

The long-term dataset indexes phytoplankton biomass in terms of chlorophyll *a*. In order to convert chlorophyll *a* to organic carbon and BOD equivalents, the phytoplankton chlorophyll *a* to carbon ratio (Chl:C) is required. Cloern et al. (1995) developed an empirical expression for this ratio dependent on temperature, mean water column irradiance, and nutrient concentration:

$$\text{Chl:C} = 0.003 + 0.0154 \left(\frac{N}{k_n + N} \right) \exp(0.050T) \exp(-0.059I_{av}) \quad (1)$$

where T ($^{\circ}\text{C}$) is water column temperature, I_{av} ($\text{mol m}^{-2} \text{d}^{-1}$) is daily photosynthetically active radiation (PAR) averaged over the mixed layer, N (mg/L) represents the concentration of the nutrient limiting growth rate, and k_n (mg/L) the half-saturation constant that defines sensitivity of growth to changes in nutrient concentration. The equation was based on 12 published studies involving 219 different growth conditions for unialgal cultures, mostly of coastal and estuarine diatoms. As discussed below, nutrient limitation rarely occurs in the Delta and especially the San Joaquin River upstream of the Ship Channel. We therefore assumed that the term $N/(k_n + N) = 1$ in this study. Assuming an exponential decline of PAR with depth and complete mixing of the water column, average PAR can be described by

$$I_{av} = \frac{I_0}{K_d H} (1 - \exp[-K_d H]) \quad (2)$$

where I_0 ($\text{mol m}^{-2} \text{d}^{-1}$) is PAR just below the water surface, K_d (m^{-1}) is the vertical attenuation coefficient for downwelling PAR, and H (m) is station depth. I_0 in (2) was based on daily irradiance for Davis, California, the nearest location for which a complete record is available (CDWR 2004). A factor of 0.18 was used to convert daily mean irradiance (W m^{-2}) to PAR quantum irradiance ($\text{mol quanta m}^{-2} \text{d}^{-1}$), assuming PAR is 45% of total irradiance and a conversion of 2.77×10^{18} quanta $\text{s}^{-1} \text{W}^{-1}$ for PAR (Morel and Smith 1974). Because K_d measurements are available only for a portion of the record (1975–1979 at Vernalis and 1975–1986 at Mossdale), we estimated K_d using the data from Mossdale and Vernalis combined ($R^2 = 0.65$, $n = 296$, $P < 0.001$):

$$\ln K_d = - (0.49 \pm 0.08) + (0.51 \pm 0.02) \ln M \quad (3)$$

where M (mg L^{-1}) refers to particulate matter as estimated by total suspended solids, and coefficient values \pm standard errors are shown explicitly. Thus, $K_d \propto \sqrt{M}$, approximately.

We also needed to estimate instantaneous values of average water column PAR in order to assess light limitation. Daylength Γ (h) was determined from latitude (Forsythe et al. 1995), and then mean *daily* irradiance was converted to mean *daylight* irradiance based on daylength.

Maximum irradiance I_{\max} ($\mu\text{mol m}^{-2} \text{s}^{-1}$) was estimated based on the ratio of maximum to mean daylight, using a simple sinusoidal light curve to describe diurnal surface irradiance (Platt et al. 1990). Average water column values were then obtained from (2).

We followed the general procedure of Reynolds and Maberly (2002) to estimate the phytoplankton carrying capacity of macronutrients. We used total nitrogen (N_{tot}) and total phosphorus (P_{tot}) to calculate carrying capacities for nitrogen and phosphorus, in order to determine maximum values and to avoid the uncertainty in estimating the bioavailable fraction of nutrients. The use of total nutrient concentration is actually necessary for the Delta data set, as total ammonia is much larger than dissolved ammonia, but only the latter has been measured routinely. Carrying capacities are therefore overestimates. The theoretical stoichiometric yield of phytoplankton cell carbon is C:N = 5.7 and C:P = 41 (Stumm and Morgan 1981). The carrying capacity in chlorophyll *a* units for nitrogen is then simply $N_{\text{tot}}(\text{C:N})(\text{Chl:C})$, and for phosphorus, $P_{\text{tot}}(\text{C:P})(\text{Chl:C})$. Our approach differs from Reynolds and Maberly's, however, in that we did not consider the Chl:C ratio to be constant. Rather, we used equations (1) and (2). Because the C:Si ratio for diatoms is so highly variable among taxa, we did not estimate a carrying capacity for silicon.

We used the derived equation of Reynolds (Reynolds and Maberly 2002) to estimate the supportive capacity of light, B_{\max} ($\mu\text{g chlorophyll } a \text{ L}^{-1}$)

$$B_{\max} = \frac{1}{\kappa} \left[\frac{0.75 P_r \Gamma}{24H} \ln \left(\frac{1.4 I_{\max}}{I_k} \right) - K \right] \quad (4)$$

where P_r is the dimensionless ratio of maximum photosynthetic rate to basal respiration rate at the same temperature, Γ is daylength (h), I_{\max} is daily maximum PAR ($\mu\text{mol m}^{-2} \text{s}^{-1}$), and I_k is PAR at the onset of light saturation ($\mu\text{mol m}^{-2} \text{s}^{-1}$). κ is the vertical light attenuation due to chlorophyll *a* ($\text{m}^2 [\text{mg chlorophyll } a]^{-1}$), and K is the non-phytoplankton-associated vertical light attenuation (m^{-1}). They are related to the vertical attenuation coefficient K_d (m^{-1}) as follows

$$K_d = \kappa B + K \quad (5)$$

We used the parameter values suggested by Reynolds and Maberly (2002): $\kappa = 0.01$, $P_r = 15$, and $I_k = 20$. Γ and I_{\max} were determined as above. K was estimated from (5). There is much uncertainty in the parameter values chosen by Reynolds and Maberly (2002) and so estimates of B_{\max} cannot be considered very reliable. Although there are other ways to arrive at maximum biomass estimates, they all suffer from a similar uncertainty.

Growth rate estimates are required to understand the demands on nutrient resources in transit to the Ship Channel. We know that daily gross primary production P ($\text{mg C m}^{-2} \text{d}^{-1}$) is described well in the Delta by

$$P = 4.61 \frac{\Psi B I_0}{K_d} \quad (6)$$

where Ψ ($\text{mg C} [\text{mg chlorophyll } a]^{-1} [\text{mol m}^{-2}]^{-1}$) is the water column light utilization efficiency and B ($\mu\text{g/L}$) is chlorophyll a concentration. This relationship is based on theoretical considerations for low light conditions and has been shown experimentally to apply to Delta primary productivity (Cole and Cloern 1987). It follows that net (geometric) growth rate r (d^{-1}) can be expressed in terms of P by

$$r = (1 - \rho_0) \frac{P (\text{Chl:C})}{B H} - \rho_1 = 4.61 (1 - \rho_0) \Psi (\text{Chl:C}) \frac{I_0}{K_d H} - \rho_1 \quad (7)$$

where respiratory losses are divided into a photosynthesis-dependent fractional loss ρ_0 and a basal metabolic loss ρ_1 (d^{-1}). The term $(\text{Chl:C})/H$ simply converts volumetric chlorophyll a concentrations B into areal carbon concentrations. The right-hand side has been written to emphasize the physical interpretation: $\Psi(\text{Chl:C})$ is the efficiency with which light is manifested as growth rate, and $I_0/K_d H$ is the mean light in the water column assuming, as in the San Joaquin River, that essentially all light is absorbed before the bottom. The efficiency Ψ is taken to be 0.73 (Jassby et al. 2002). Values for the respiration parameters are based on the study of Cloern et al. (1995), who summarized empirically the results of many experiments in the literature in which both photosynthesis and growth rates were measured: $\rho_0 = 0.15$ and $\rho_1 = 0.015$. The estimation of Chl:C is also based on the latter study, as described above.

2.3 Hydrological Estimates

Values of net discharge into the Ship Channel are also necessary to estimate phytoplankton demands on river nutrients. The U.S. Geological Survey has operated an Ultrasonic Velocity Meter (UVM) station in the San Joaquin River just upstream of the Ship Channel (<http://sfbay.wr.usgs.gov/access/delta/tidalflow>; Figure 2). A 15-minute interval UVM tidal flow record is computed and converted to discharge using water-surface elevation, channel geometry survey data, and Acoustic Doppler current profiler measurements. The station has only been in operation since August 1995. The best estimate of historical mean daily flows in the Delta is obtained with Dayflow, a computer program developed in 1978 as an accounting tool for determining historical Delta boundary hydrology (IEP 2003). Dayflow output itself does not contain estimates of discharge into the Ship Channel, but the question naturally arises as to whether a surrogate net flow series can be constructed by determining a relationship between net discharge and Dayflow variables. The largest effects on tidally-averaged net flow should be the upstream flow in the San Joaquin River and the split in flow taking place at the head of Old River. The latter is driven by exports from the Delta into the federal Central Valley Project and State Water Project. Estimates of San Joaquin River discharge at Vernalis and of exports are available from Dayflow output (<http://iep.water.ca.gov/dayflow/index.html>). Net flow is also affected by the presence of a temporary rock barrier—the Head of Old River barrier—constructed annually at the confluence of the Old and San Joaquin rivers to protect outmigrating juvenile salmon from the federal and state pumping plants (http://sdelta.water.ca.gov/web_pg/tempmesr.html). The barrier has been in place most years since 1963 between September 15 and November 30. It was also installed in the spring between April 15 and May 30 of 1992, 1994, 1996, 1997, 2000, 2001, 2002, and 2003. We created a monthly variable B_{hor} equal to the proportion of the entire month during which the barrier was in place (we assumed that the barrier was in place from the installation completion date until the removal completion date). Net flow was estimated by

$$Q_{net} = c_0 + c_1 Q_{vern} + c_2 Q_{xport}(1 - B_{hor}) \quad (8)$$

where Q_{net} (m^3/s) is monthly mean net flow into the Ship Channel, Q_{vern} (m^3/s) is monthly mean flow at Vernalis, Q_{export} (m^3/s) is monthly mean water export from the Delta, and B_{hor} is the state of the Old River barrier. The effect of this barrier is complicated by the addition of culverts in recent years that allow some flow through the barrier, and by temporary rock barriers installed further downstream on Old River to increase water levels in south Delta sloughs, primarily for agriculture diversions. Neither complication is reflected in B_{hor} .

We use the San Joaquin Valley Water Year Hydrologic Classification, which identifies each water year as one of five types, depending on unimpaired discharge: critical, dry, below normal, above normal, and wet. Exact definitions and data can be accessed at <http://cdec.water.ca.gov/cgi-progs/iodir/wsihist>. A water year extends from October 1 of the previous calendar year through September 30. Unimpaired discharge refers to summed discharge upstream of dams on the San Joaquin drainage system.

2.4 Data Analysis

Unless otherwise stated, replicate samples for all variables have been averaged and data within the same month aggregated by their median, in order to avoid bias when comparing seasons with different amounts of raw data. When necessary, small gaps in monthly time series were imputed using a time series modeling procedure known as TRAMO (Time series Regression with ARIMA noise, Missing observations, and Outliers; Gómez and Maravall 2002), which retains the autocorrelation structure in the series. When assessing trends by month in time series, a robust measure—sometimes known as the Theil trend—is used. This is simply the median slope of the lines joining all pairs of points in the series. The Kendall-tau test can be used to determine the significance of the trend (Helsel and Hirsch 1992).

Principal component analysis (PCA) of monthly time series was used to investigate interannual variability (Jassby 1999). PCA time series analysis reveals the number of independent underlying modes of variability, the time of year in which they are most important, and their relative strength from one year to the next. These features often provide strong constraints on the underlying mech-

anisms while also providing clues for their identity. The time series is first reshaped into a years \times months data matrix. Principal components (PCs) were estimated by singular value decomposition of the covariance matrix of the data matrix. The number of significant PCs was chosen using a Monte Carlo technique known as Rule N.

Restricted cubic splines were used as transforms for predictors in regression relationships (Harrell 2001). A cubic spline is a piecewise polynomial of order three that is smooth (specifically, it has continuous first and second derivatives) at the knots (i.e., points joining the different polynomial pieces). A restricted cubic spline or natural spline is further constrained by being linear beyond the outer knots. The use of splines in general and restricted cubic splines in particular has many advantages over other methods in representing nonlinear functions in a regression model when the exact form of the nonlinearity is unknown. To minimize the number of parameter estimates, we used a restricted cubic spline with only three knots, requiring only two parameters. The knot positions—at the 0.1, 0.5, and 0.9 quantiles—were chosen based on general recommendations from simulation studies, and were not tailored in any way for the current data set. The spline functions can therefore be described in general by

$$f(x) = b_1x + b_2[(x - k_1)_+^3 - (x - k_2)_+^3(k_3 - k_1)/(k_3 - k_2) + (x - k_3)_+^3(k_2 - k_1)/(k_3 - k_2)] \quad (9)$$

where b_1 and b_2 are constant coefficients, the k_i are the 0.1, 0.5, and 0.9 quantiles of x , and

$$y_+ = \begin{cases} 0 & y \leq 0 \\ y & y > 0 \end{cases} \quad (10)$$

Overfitting in regression models refers to distorted parameter estimates (and predictions) that can result from a small ratio of observations to predictors. Overfitting was estimated by using the 0.632 bootstrap estimator of prediction error (Efron 1983) to produce corrected values of R^2 . In this method, the model is refitted many times using bootstrap samples of the original observations.

For each bootstrap sample, observations not included in the sample are compared with model predictions. The average error rate is then calculated for each observation over all bootstrap samples, and an overall error rate is determined by averaging over all observations. Based on theoretical considerations, the prediction error can then be estimated from the original R^2 and the overall average error rate. Bootstrap samples of 2000 were used, sufficient for at least two significant digits. Harrell (2001) describes the bootstrapping algorithm used here.

Multivariate regression model results are illustrated as partial residual plots, which attempt to show the relationship between a given independent variable and the response variable, while accounting for the other independent variables in the model. Specifically, a partial residual plot here refers to a plot of $r_i + b_k x_{ik}$ versus x_{ik} , where r_i is the ordinary residual for the i -th observation, x_{ik} is the i -th observation of the k -th predictor, and b_k is the regression coefficient for the k -th predictor.

3 Results

3.1 Historical Time Series

Interannual variability in chlorophyll a is strong (Figure 3). Phytoplankton at both Vernalis and Mossdale can reach very high concentrations, up to 337 $\mu\text{g/L}$ in August 1977 during the extreme dry El Niño-Southern Oscillation event (ENSO) of 1976–1977. At the other extreme, concentrations remained below 10 $\mu\text{g/L}$ the entire year during the extreme wet event of 1983. A principal component analysis of the Vernalis time series demonstrated that there was only one significant mode of interannual variability, accounting for 72% of the overall variability (Figure 4A). This mode was centered in June–August, the period when phytoplankton almost always reaches its annual maximum (Figure 4B), although there is one case each of May (1983), September (2000), and October (1991). Interannual variability is thus determined by the size of the annual chlorophyll a peak, and the time series of maximum annual chlorophyll a concentrations contains almost as much information as the time series of monthly values. We therefore focused on understanding

regulation of the annual chlorophyll *a* peaks.

The seasonal pattern also reflects precipitation and runoff, with lowest values typically in December–January during the wet season, and highest values typically in July–August during the dry season (Figure 3). The maximum biomass at Mossdale was typically higher than at Vernalis by a mean of $32 \pm 8\%$. Only 4 of 21 years showed a downstream decrease: 2 of these were the extreme dry years 1977 and 1992, and all 4 showed a decrease of less than 5%. The phytoplankton is thus usually in its (longitudinal) increasing phase in this reach. The summer biomass peaks at the Vernalis and Mossdale stations were almost always dominated by small centric diatoms characteristic of turbid, well-mixed rivers, most commonly of the genera *Cyclotella* and *Thalassiosira* (20 of 27 years, 1975–2001). Leland et al. (2001) found similar dominants in their four-year study of algal species composition in the perennial San Joaquin River upstream of Vernalis, implying a continuity of the main populations along the mainstem.

3.2 Resource Constraints on Carrying Capacity and Growth Rates

In order to determine if resource availability controlled phytoplankton biomass, the carrying capacity for each macronutrient and for incident light was estimated for the time when annual peak chlorophyll *a* occurred. We used data for Mossdale, because biomass usually increases between Vernalis and Mossdale and approaches carrying capacity more closely at the latter station. Carrying capacities are surprisingly similar for the macronutrients and light (Figure 5). On average, observed peak chlorophyll *a* values reach only a small percentage of the carrying capacity, from 10% (light) to 13% (phosphorus). They are also less than 50% of carrying capacity in almost all years for each resource. In the extreme dry years such as 1976–77 and 1991–92, however, they can be more than 50% of carrying capacity: The maximum percentages are 59% for light (1977), and 69% for nitrogen (1977) and 66% for phosphorus (1991). The latter suggests that most of the total nitrogen and phosphorus is actually available for phytoplankton growth, and that the use of total nitrogen and phosphorus to estimate carrying capacities does not bias the qualitative impression that macronutrients usually do not limit biomass.

Phosphorus carrying capacity was lower than nitrogen carrying capacity in 15 of 20 years, and the relative sensitivity to phosphorus limitation appears to be increasing. There is no overall upward or downward trend over the whole record for either total nitrogen or phosphorus (not shown). Indeed, although the trends for total nitrogen by month are mostly upward, and for total phosphorus mostly downward, only in one month each were the trends significant: $+0.050 \text{ mg L}^{-1} \text{ yr}^{-1}$ nitrogen in June ($P = 0.019$); and $-0.019 \text{ mg L}^{-1} \text{ yr}^{-1}$ phosphorus ($P = 0.001$) in September. In contrast, the total nitrogen to phosphorus ratio exhibits a clear rise over time (Figure 6A), and the monthly trends are significant for most of March–October, covering the main growth period for phytoplankton (Figure 6B). Values early in the record are close to the Redfield ratio of 16, typical of phytoplankton. In the last decade, however, this ratio has been exceeded almost every month.

We also investigated resource constraints on growth rate using dissolved nutrient concentrations. Nutrient limitation of phytoplankton growth typically becomes significant only when nutrient concentrations fall below about 0.07 mg/L nitrogen and 0.03 mg/L phosphorus; these values are at least five times typical half-saturation constants for uptake (Fisher et al. 1995). We examined nutrient concentration for those months in which the peak annual biomass occurred, usually during June–August, although there is one case each of May (1983), September (2000), and October (1991). At Vernalis, the minimum nutrient concentrations at those times were 0.300 mg/L dissolved inorganic nitrogen and 0.040 mg/L soluble reactive phosphorus, i.e., above the threshold for nutrient limitation. Median values were 1.67 and 0.090 mg/L , respectively. At Mossdale, the medians were similar— 1.42 and 0.085 mg/L , respectively—but soluble reactive phosphorus decreased to 0.010 mg/L in the dry years of 1976, 1977, and 1991, and dissolved inorganic nitrogen was as low as 0.110 in both 1991 and 1992. It is therefore possible that nutrient limitation occurs at Mossdale in extreme dry years. But this must be more the exception than the rule because nutrient levels are usually much higher than the thresholds for limitation even at Mossdale. Moreover, the routine measurements include only dissolved ammonia and there may be considerable available ammonia attached to mineral particles. Similarly, soluble reactive phosphorus may underestimate

available phosphorus because of uncertainty about intracellular storage and other dissolved fractions (Bradford and Peters 1987).

Although carrying capacities for silicon cannot be estimated with any certainty, the dissolved concentrations are informative. The median value for silicon at Mossdale during 1975–1995 was 15 mg/L and the absolute minimum (1977) was 1.2 mg/L silica. In lakes, silicon limitation does not occur until silica concentrations drop well below 1 mg/L (Lund 1964). In marine diatoms, Azam and Chisolm (1976) found half-saturation constants of 0.15 mg/L silica or less for silicic acid uptake. Kilham and Kilham (1975) argued on the basis of distributional data that *Aulacoseira granulata* grows best where silicon is not limiting, and this species is often abundant in the San Joaquin River. Silicon limitation of growth rate is thus highly unlikely. Even if diatom biomass at Mossdale did become limited by silicon availability in extreme droughts, non-diatoms would then simply have the advantage and in principle could take over a dominant role at those times. We will therefore focus on nitrogen and phosphorus in what follows.

We examined light conditions in the water column at the time of peak biomass each year. Average water column irradiance at the time of maximum daily irradiance ranged from 53 to 195 $\mu\text{mol m}^{-2} \text{s}^{-1}$ over the years, with a median of 91. In comparison, characteristic values for the irradiance level promoting maximum primary productivity are usually in the range 200–800 $\mu\text{mol m}^{-2} \text{s}^{-1}$ (Padisák 2004). Note that these average water column irradiances are *maximum* daily values. Average daily values are only 64% of the maximum, assuming a sinusoidal light curve, and so phytoplankton growth rate in the San Joaquin River is probably light-limited at the time of the annual phytoplankton peak. Growth rate at Mossdale during times of peak phytoplankton biomass were estimated using (1) and (7). Geometric growth rates are mostly in the range 0.3–0.6 d^{-1} , equivalent to exponential growth rates of 0.2–0.4 d^{-1} (Figure 7). As pointed out above, nutrient limitation may have been present at Mossdale in 1976–77 and 1991–92, in which case $N/(k_n + N) < 1$ in (1) and growth rates would have been lower.

Note that light attenuation is usually due mostly to mineral suspensoids, as opposed to phytoplankton. Phytoplankton contributes little, on average, to total suspended matter at Mossdale, even

at peak annual biomass. For example, assuming a Chl:C ratio given by (1) and a characteristic carbon to dry weight ratio of 0.3 for a community containing diatoms and non-diatoms, the median contribution during the annual peak was 12% (1975-1995). Contributions during extreme dry years can be much higher, though, as high as 45% in 1977. Using a typical value of $0.01 \text{ m}^2 [\text{mg chlorophyll } a]^{-1}$ for PAR attenuation, the chlorophyll *a* contribution to observed K_d at Mossdale was a median of only 14% but reached as high as 82% in 1977 (1975–1985). The very dry years thus favor high chlorophyll *a* concentration even more than high total suspended solids.

3.3 Phytoplankton Biomass and River Discharge

San Joaquin River discharge appears to be a dominant controlling factor for chlorophyll *a* concentrations at Vernalis and Mossdale. This can be appreciated by comparing monthly chlorophyll *a* concentrations with discharge rates (Figure 3). Peak annual values of chlorophyll *a* appear to be determined by discharge rates during the summer. For example, the two peaks over $300 \mu\text{g/L}$ in 1977 and 1992 correspond to the two lowest discharge values. In the early years of the 1987–1994 drought, summer discharge remained relatively high and peak values correspondingly low. As summer discharge declined throughout the drought, summer chlorophyll *a* increased. In fact, the disappearance of high chlorophyll *a* values after 1977 until the early 1990s can be understood based on summer discharge rates alone. Figure 8 illustrates the relationship between annual maximum chlorophyll *a* and discharge during the same month. Vernalis data are used because they are available for a longer time period. Peak chlorophyll *a* increases dramatically as concurrent discharge decreases. There is some indication of a rapid rise below about $50 \text{ m}^3/\text{s}$, and a (weak) suggestion of saturation at the highest chlorophyll *a* level in 1977.

There is much variability in the relationship at intermediate discharge values. Much of this variability appears to be due to a change in the relationship over the years, with earlier chlorophyll *a* observations tending to be higher for a given discharge level. We explored the different behavior in early compared to later years by modelling chlorophyll *a* as a function of discharge and time. Based on Figure 8, we assumed a power relationship between chlorophyll *a* and discharge, with

the addition of a time trend. In order to allow the data themselves to determine the form of the trend, we modeled the trend as a restricted cubic spline transform of time. Only three knots were used for the spline, requiring only two additional coefficients to be estimated:

$$\ln(B) = a_1 + a_2 \ln(Q_{vern}) + f(T) + \epsilon_t \quad (11)$$

where B is chlorophyll a , Q_{vern} is discharge at Vernalis, T is the year, f is the spline-estimated transform of year, a_1 and a_2 are constant coefficients; and ϵ_t is an independent normal process. The spline function is given by (9).

The residuals are free of serial correlation and approximately normal. All variables are important according to the partial F tests, including the nonlinearity in the trend (Table 1). The adjusted $R^2 = 0.83$. Because of concern about overfitting when estimating three coefficients (apart from the intercept) from only 34 observations, we used a bootstrap method to determine corrected R^2 estimates that are more realistic when the model is used to predict new observations. The corrected R^2 fell to only 0.80, indicating that overfitting is minor. Although we would have preferred to use a spline transform for Q_{vern} as well, the bootstrap calculations demonstrated that this would lead to serious overfitting, with R^2 dropping from 0.90 to 0.60. In any case, the results indicate an approximate power relation between chlorophyll a and river discharge ($B \propto Q_{vern}^{-0.76}$), with the effect of a given discharge value less in later versus early years (Figure 9). Although there is some hint of an upturn in recent years, the standard errors indicate that it lacks statistical significance. The trend is constrained to be smooth because the data allow only one interior knot, but the partial residuals for the trend suggest that an abrupt drop may have happened around the 1976–77 ENSO.

July discharge during drought years has increased in recent decades (Figure 10). Before 1980, July discharge during critical and dry years was always below 20 m³/s. Since 1980, discharge for these water year types fell below this threshold only towards the end of a six-year drought in 1992. Median discharge for critical years was 4.6 m³/s before 1980, and 32 m³/s since that time; discharge for dry years was 12 and 38 m³/s, respectively. At least part of this increase

is due to changes in the Stanislaus River since the New Melones Dam began operation on the river in 1979 (Figure 1). One of the dam's functions is to decrease Delta salinity intrusions during summer by providing auxiliary flow to the San Joaquin River. Since dam completion, the Stanislaus has contributed a median of 33% of the San Joaquin discharge in July. This increase in summer flow from the San Joaquin is due to a shifting seasonal pattern of storage and release. Figure 11 illustrates how July discharge from the Stanislaus River has increased as a proportion of total annual Stanislaus discharge. The median value for July was 2.7% of annual discharge before the dam was established, and 7.1% after.

Discharge affects phytoplankton biomass not only through transit time but also through growth rate, because of changes in light attenuation due to discharge impacts on suspended matter. The relationship between suspended matter and discharge depends on the season. Suspended matter decreases with flow for any given month from late winter to early fall, but not during the remaining months (Figure 12). April and December show strongly opposite relationships with discharge. Although the correlation with discharge is significant for March–July and December, most of the variability appears to be due to other factors. The variability explained by discharge in July, for example, is $R^2 = 0.29$. The dependence of suspended matter on discharge is also much weaker than the inverse dependence of transit time on discharge. The exponent of the power relationship in July, for example, is only -0.23.

3.4 Net River Discharge and Export Effects

Water exports via Old River decrease river discharge downstream of Mossdale. Net discharge Q_{net} below this point was estimated using (8). This model describes the overall data well, and is also well-behaved statistically (Figure 13, Table 2). The value of adjusted $R^2 = 0.93$, and the residuals are not serially correlated. The model describes the low-flow data less well than the entire dataset. We refit the model using only data for $Q_{net} < 85 \text{ m}^3/\text{s}$. The overall fit was, of course, poorer, but the fit for low-flow data did not improve. The lack of fit for low values probably represents physical processes missing from the model and cannot be corrected solely through statistical means. The

overestimation of low flows by the model could possibly be remedied by the inclusion of a term representing culverts through the Head of Old River barrier. Diversion of water for irrigation downstream of the Old River branch may also play a role. In any case, we considered the model adequate for the application at hand. As net discharge should be less than or equal to discharge at Vernalis, we used the smaller of Q_{net} and Q_{vern} to represent net discharge. Travel times between Mossdale and the Ship Channel were estimated from discharge using a relationship developed by Jones & Stokes (2002) for this reach of the river. Travel time estimates assume zero tidal dispersion but, in reality, transit times could be shorter or longer in the tidal river.

Mossdale is 26 km from the entrance to the Ship Channel, so there is further opportunity for phytoplankton growth between Mossdale and the Ship Channel. It is interesting to consider the impact of flows down Old River on phytoplankton growth over this distance. At the time of peak phytoplankton concentration, travel times averaged 2.1 ± 0.4 days during 1975–1995, ranging from 0.099 in 1983 to 8.4 in 1977. If the barrier at the head of Old River had been in place and completely effective during this time, travel times would have averaged 1.4 ± 0.4 days. Some idea of the potential effects on phytoplankton biomass can be obtained by using the growth rates estimated for Mossdale, although these could change on the way downstream and nutrient or light resources could become limiting before phytoplankton reached the Ship Channel. Note also that water within a few kilometers upstream of the Ship Channel is subject to mixing with Ship Channel water because of tidal dispersion, so that concentrations in this region do not reflect the true net increase in biomass of a population starting out at Mossdale. With this understanding, we calculated that the effect of water diversions down Old River is to increase peak biomass during 1975–1995 at the Ship Channel by a mean of $38 \pm 10\%$, with a maximum increase of 140% in 1989. In three of the driest years—1977, 1991, and 1992—exports were negligible. In other years, however, the effect of exports down Old River could have been a notable increase in the concentration of phytoplankton biomass downstream. In 1989, for example, potential downstream concentrations at the time of the peak would have been only $73 \mu\text{g/L}$, instead of $177 \mu\text{g/L}$ (potential concentrations assume no dilution of the biomass with Ship Channel water).

4 Discussion

4.1 Nutrient Management and Phytoplankton

The concentrations of dissolved inorganic nitrogen, soluble reactive phosphorus, and dissolved silica indicate that macronutrient limitation is unlikely at Vernalis or Mossdale, except perhaps during extreme drought years (such as 1976–77 and 1991–92). Apart from these extreme years, though, nutrient concentrations do not appear to restrict either phytoplankton growth rate or biomass. There is much uncertainty in the estimates made here. For example, phytoplankton chlorophyll *a* can vary several-fold over the diel cycle (Reynolds 1997) and is known to have a two-fold diel variation at continuous monitoring stations on the San Joaquin River. In addition, total elemental concentrations overestimate carrying capacity. Yet Figure 5 illustrates a large enough difference between estimated biomass and carrying capacities that the conclusion is a robust one. Whether the situation changes in transit to the Ship Channel, i.e., whether phytoplankton achieve carrying capacity in more than just extreme dry years, remains in question because of probable changes in growth rate, losses to primary consumers, and downstream losses or gains in total elemental concentrations. There are insufficient long-term data between Mossdale and the Ship Channel to address the question. Moreover, water just a few kilometers upstream of the Ship Channel is subject to dilution because of tidal dispersion. The effects of phytoplankton growth in transit downstream could therefore easily be swamped by the much lower phytoplankton concentrations in the Channel for measurements made in the vicinity of the Channel.

Which of nitrogen or phosphorus would require the smallest reduction to achieve nutrient limitation, i.e., which nutrient is more liable to be limiting in the San Joaquin River? The N:P molar ratio for phytoplankton averages 16, but Downing and McCauley (1992) found that nitrogen rather than phosphorus limitation (albeit in lakes) was significantly more frequent until total N:P exceeded 31. The ratio at Vernalis is typically below this threshold (median 18) and sometimes even below 16. Dissolved inorganic N:P values are substantially higher (median 27), but it is difficult to interpret this ratio in the San Joaquin River: ammonia bound to particles, despite its proba-

ble availability, is substantial but not included in routine ammonia measurements. Also, here as elsewhere, the true availability of phosphorus can be underestimated because of internal cellular storage. The ratios are therefore in a band where interpretation is uncertain and we cannot conclude definitely that the river is more prone to either nitrogen or phosphorus limitation. It is not uncommon for estuarine phytoplankton communities to be prone to colimitation by nitrogen and phosphorus (Conley 2000), and the same tendency may characterize this tidal reach of the San Joaquin River. In any case, the long-term trend for both total N:P (Figure 6) and inorganic N:P values since 1980 has been in the direction of higher ratios and more susceptibility to phosphorus limitation.

Kratzer and Shelton (1998) have noted a long-term increase in nitrate concentration in the San Joaquin River, which they attributed to native soil nitrogen from expanding subsurface agricultural drainage. More recently, Kratzer et al. (2004) observed that all but a few $\delta^{15}\text{N}$ and $\delta^{18}\text{O}$ values of nitrate measured in the San Joaquin River fell within the range of animal waste and sewage. They concluded that animal waste or sewage now represented a significant source of nitrate in the San Joaquin River at the time of sampling. During the summer and early autumn when the study took place, higher temperature and travel times from sources favor conversion of dissolved organic nitrogen and ammonia to nitrate. Consistent with these observations, Kratzer and Shelton (1998), in their earlier study of 1972–1990 water quality, reported that about 53% of total nitrogen sources in the drainage basin for the San Joaquin River near Vernalis consisted of manure production. The nitrate increase could therefore be due, at least in part, to an increase in animal waste and sewage sources. Other changes possibly affecting the nitrogen and phosphorus balance over time include an increase in aeration of municipal wastewater ponds and land application of domestic wastewater.

How much reduction in nitrogen or phosphorus is required to induce nutrient limitation? It is difficult to provide a general answer to this question, because nutrient and suspended sediment loading is year-dependent, and peak biomass depends on water year type and seasonal patterns of storage and release from impoundments. Downstream of Old River, it also depends on water exports. Figure 5 however, does provide an answer from a historical perspective: at peak biomass,

phytoplankton reached an average of $21 \pm 4\%$ of nitrogen and $23 \pm 4\%$ of phosphorus carrying capacity, requiring reductions of at least 75% to have an effect. Moreover, this is the minimum reduction required to induce limitation: it does not tell us how much reduction is necessary to limit phytoplankton biomass to acceptable levels. For that, a specific goal is needed. Consider, for discussion purposes, the OECD (1982) boundary between mesotrophy and eutrophy of $25 \mu\text{g/L}$ maximum annual chlorophyll *a*. Reductions of this amount probably would not affect the algal food supply to planktonic food webs, which appear to be saturated at a level of $10 \mu\text{g/L}$ chlorophyll *a* (Müller-Solger et al. 2002). Depending on the year, the $25 \mu\text{g/L}$ goal would have required reductions of 74 to 97% for nitrogen or 81 to 97% for phosphorus. These are very challenging amounts. Any nutrient control therefore should have some beneficial effect, but levels of nutrient reduction attainable in the short term will probably leave peak phytoplankton biomass unchanged in many years.

4.2 Light-Attenuating Materials

Historical year-to-year changes in mineral suspensoid concentrations in the San Joaquin River, unlike macronutrient changes, probably had important effects on phytoplankton growth and biomass. Average light levels experienced by phytoplankton are relatively low and neither photosynthesis nor growth rate are proceeding at maximum attainable levels. Total suspended solids in July has ranged from 38 mg/L in 1998 to 226 mg/L in 1976. Even considering that $K_d \propto \sqrt{M}$, this represents about a 2.4-fold change in growth rate, according to (7). Although this includes year-to-year variability in the phytoplankton as well as mineral suspensoid portion, the latter must still be considerable given that phytoplankton accounts for a minority of suspended matter during the annual peak. The implication is that watershed or river management actions must reflect an understanding of the consequences for mineral suspensoids in the river. For example, dam removal may decrease transparency by eliminating trapping of suspended matter in reservoirs. On the other hand, erosion control measures for fine-grained soils from the Coast Range on the west side of the Valley or for agricultural lands on the east side may increase transparency. Growth rate and even bio-

mass could increase if nonpoint source management decreases mineral suspended load but does not decrease nutrient load sufficiently. The effects can be very large: Reservoirs in Germany and Austria decreased suspended matter and improved water clarity in the Danube River during the 1970s, resulting in a ten-fold increase in phytoplankton with no change in nutrient supply (Kiss 1994). Transparency responses should be an explicit component of models intended for assessing different strategies to manage loads to the Ship Channel.

4.3 River Discharge

River discharge during June–August has the strongest identifiable effect on peak phytoplankton biomass at Vernalis. Although phytoplankton may reach the carrying capacity set by macronutrients during extreme drought years, it is usually well below this capacity. Growth rate is light-limited due to high levels of mineral suspended solids, compounded by high nutrient levels that permit phytoplankton to reach densities of at least $336 \mu\text{g/L}$ at Vernalis, values near the top of the range found in rivers. Maximum phytoplankton biomass therefore depends primarily on river discharge, which determines the cumulative light exposure in passage to Vernalis. Based on historical evidence, maintaining river discharge above $50 \text{ m}^3/\text{s}$ during early summer would eliminate large blooms at Vernalis. Downstream of Mossdale, however, export flows down Old River can further reduce mainstem river discharge, and further increase the cumulative light exposure in passage to the Ship Channel. These export flows may result in more than a doubling of peak biomass at the entrance to the Ship Channel in individual years.

Discharge also affects total suspended solids and therefore light-limited growth rates, apart from its effects on cumulative light exposure through residence time (Figure 12). The relationship between suspended matter and discharge during summer implies a positive effect of discharge on biomass by increasing growth rate, in addition to an opposing negative effect by decreasing residence time. The latter linkage is the dominant one by far, however. As pointed out in the Results, total suspended solids $M \propto Q^{-0.2}$, approximately, during June–August (Figure 12). Because $K_d \propto \sqrt{M}$ (3), a doubling of discharge thus leads to an increase of only about 7% in growth rate,

according to (7). Consider a biomass of $100 \mu\text{g/L}$ chlorophyll *a*, a growth rate of 0.4 d^{-1} , and a transit time of 2 days to some second location downstream. The net affect of doubling discharge is to decrease biomass at the downstream location from 196 to $143 \mu\text{g/L}$. Without any effect on growth rate, final biomass would have been $140 \mu\text{g/L}$, a negligible difference. In other words, secondary optical effects can probably be ignored when considering how flow affects phytoplankton biomass within any given season.

The huge interannual excursions in phytoplankton biomass for the San Joaquin River (Figure 3) can be remarkably well understood simply on the basis of discharge. A key point, however, is that peak annual biomass is only loosely connected to total annual precipitation. Rather, it depends on concurrent discharge in the early summer (Figure 9A). Because of impoundment patterns of water storage and release, the seasonal hydrograph has shifted to lower discharge in spring and higher discharge in summer (Knowles 2002). During the early years of the 1986–1992 drought, peak biomass remained relatively low, despite the overall dry conditions. This change from earlier drought years such as 1976–77 appears to be due simply to the fact that discharge remained elevated and residence times accordingly low during early summer. The change in median July discharge from 4.6 and $12 \text{ m}^3/\text{s}$ during critical and dry years, respectively, before 1980, to 32 and $38 \text{ m}^3/\text{s}$ since 1980, falls mostly within the most sensitive portion of the chlorophyll *a*-discharge relationship (Figure 8). About half of this increase can be attributed to the changed pattern of storage-and-release on the Stanislaus River with construction of the New Melones Dam.

Although most of the interannual variability in biomass is directly attributable to differences in early summer discharge, a long-term shift in the relationship between biomass and discharge can also be observed (Figure 9B). The shift accounts for relatively little of the overall year-to-year variability but is statistically significant (Table 1), and ecologically significant for intermediate discharges of $30\text{--}50 \text{ m}^3/\text{s}$ (Figure 8). What is the mechanism behind this shift? It is possible that operation of the New Melones Dam has an effect on bloom size apart from the impact of concurrent discharge. This is especially true if lagged discharge effects are also important, because winter and summer discharge was generally much higher prior to 1980. Abundances of planktonic grazers

with generation times longer than planktonic algae are likely to be dependent on these earlier discharges. Pace et al. (1992), for example, found that advective transport regulates zooplankton biomass in the Hudson River and in other tidal rivers, estuaries, and lakes where the appropriate data could be found. Gosselain et al. (1998), however, maintain that planktonic grazing pressure on phytoplankton is unlikely to be important during low river residence times, such as in spring. In any case, we could find no convincing statistical evidence for lagged effects, and zooplankton data are not routinely collected in this reach.

A climate regime shift in the eastern Pacific and contiguous Americas occurred around 1976 (Trenburth and Hurrell 1994), coincident with major step-like changes in chlorophyll, salmon, crabs, and many other environmental variables (Ebbesmeyer et al. 1991). Lehman (2000) has suggested that this climate regime shift also had impacts on the Delta's phytoplankton community. The main effect of climate change on the San Joaquin River, however, is a change in the discharge hydrograph, which should already be accounted for by the discharge term in (11). As we have seen, the disappearance of large blooms in dry years after 1976–77 appears to have nothing to do with a climate regime shift, but rather with changes in water management. This part of the estuary is relatively poorly studied in terms of metazoa, and it is possible that the 1976–77 ENSO event itself had unobserved impacts on primary consumers, especially benthic macroinvertebrates. River depths of about 3 m in this reach are compatible with intense benthic-pelagic coupling and major impacts of benthic suspension feeders on planktonic communities. Given the continuity of the Vernalis with the upstream phytoplankton, based on taxonomic composition and chlorophyll *a* concentrations, the impact could have been on the upstream community. Elsewhere in the estuary, persistent (multi-year) low flows have allowed upstream colonization by marine benthic macroinvertebrates, such as *Mya arenaria* during the 1976–77 drought (Nichols 1985). The drought beginning in 1986 allowed invasion of Suisun Bay by an Asian corbulid clam, resulting in persistently lower phytoplankton primary production (Alpine and Cloern 1992). Again, though, relevant long-term data are not available for this reach, and recent surveys suggest that clams are currently not abundant enough to control phytoplankton concentrations (J. Thompson, U.S. Geological Survey, pers.

comm.).

The remarkable sensitivity of peak phytoplankton biomass to early summer discharge is both a liability and an opportunity. Knowles and Cayan (2002) used projected temperature anomalies from a global climate model to drive a model of watershed hydrology for the San Francisco Estuary. They estimated that, by 2090, spring runoff could be reduced by 20% of historical annual runoff, with associated increases in winter flood peaks. According to Figure 8, large increases in bloom size would be expected for flow decreases within the range of 10–50 m³/s. For the same reasons, relatively small changes in water storage and release patterns due to dam operation have a profound influence on bloom magnitude. Storage-and-release management therefore offers a potential approach for management of blooms, at least upstream of the head of Old River. In particular, flows above 50 m³/s during parts of June–August should suppress large blooms. The exact timing could be refined by following bloom development during this period at the Mossdale continuous fluorescence monitoring station. Our analysis also shows that management of water exports historically has had additional large effects below this location but—because estimates of actual biomass downstream of Mossdale are so uncertain—it is difficult to link exports to bloom size quantitatively from the historical data alone.

4.4 Concluding Remarks

The observations and analyses in this study lead to a specific conception of bloom control in this critical reach of the tidal San Joaquin River, summarized by the cause-and-effect diagram of Figure 14. It is a minimal conception in the sense that we did not have sufficient data to include primary consumer effects in our study, and these may play a big role. Nor do we consider changes in phytoplankton species community composition, which may determine, among other things, the magnitude of light-limited growth rates. Climate, water management, and watershed material inputs are the ultimate causes in the conception illustrated here. The amount of water available in spring and early summer depends on the wet season climate, but the temporal pattern depends on dam operations, which are operated in a manner that suppresses seasonality and enhances early

summer relative to spring flow. Combined, these two factors determine the actual magnitude of early summer discharge. Discharge then affects another hydrological property, average residence time in any reach of the river; average residence time downstream is further effected by water exports down Old River. Discharge also affects two water quality properties, the concentrations of suspended matter and of macronutrients. Both are also affected by variable watershed inputs, and suspended matter in addition can be affected by feedback from phytoplankton biomass in dry years when biomass is very high. Suspended matter concentrations affect growth rate, which is usually light- and not nutrient-limited. Macronutrients determine carrying capacity or maximum possible biomass, which may be attained during extremely dry years. For most years, however, bloom size is set by residence time and specific growth rate. Of these, residence time has the most sensitive link to discharge. Reductions of macronutrient inputs from the watershed would increase the percentage of years in which blooms are limited by carrying capacity, but order-of-magnitude reductions are required and these would probably not be obtainable in the near-term for social as well as logistical reasons. Moreover, strategies for macronutrient reduction from the watershed must consider accompanying impacts on suspended matter inputs from the watershed, which could result in higher growth rates and larger blooms during years when carrying capacity is not reached. In contrast, the great sensitivity of bloom size at Vernalis to early summer discharge, and the effect of water exports on phytoplankton biomass as it moves downstream, offer effective, near-term management tools. In both cases, modification of the seasonal pattern rather than changes in the overall annual amount may be sufficient to control large blooms.

How general is this conception? In systems with a different ratio of reach length to residence time, the amount of time for biomass to increase and the frequency of carrying capacity-limitation would change, but the structure of the cause-and-effect diagram would remain the same. Other differences among systems, however, do change the structure. We have already pointed out a possible additional role for benthic macroinvertebrates, known to be important elsewhere in this estuary and in many other tidal rivers; a negative linkage would then connect primary consumers to biomass. The concentrations of mineral suspensoids also have a profound structuring effect on

cause-and-effect linkages. If suspensoids were much higher, then the carrying capacity would be set by light and not nutrients, in which case a negative linkage would connect suspended matter to carrying capacity. In other words, the particular cause-and-effect structure described here has limited generality. Nonetheless, it is interesting to ask how many, or rather how few, of these diagrams are needed to classify the causal structure of tidal rivers, as part of a systematic approach to a more general conception of phytoplankton biomass management.

5 Acknowledgments

I gratefully acknowledge support for this research from the California Bay-Delta Authority (contract numbers 4600001642 and 4600002881). I also thank Jim Cloern, Lisa Lucas, and Erwin Van Nieuwenhuysse for helpful comments on the manuscript, Peggy Lehman and Peter Smith for providing essential information, and Charles Kratzer for permission to use and modify the San Joaquin Basin map.

6 References

Alpine AE, Cloern JE. 1992. Trophic interactions and direct physical effects control phytoplankton biomass and production in an estuary. *Limnology and Oceanography* 37:946-955.

Azam F, Chisholm SW. 1976. Silicic acid uptake and incorporation by natural marine phytoplankton populations. *Limnology and Oceanography* 21(3):427-435.

Basu BK, Pick FR. 1996. Factors regulating phytoplankton and zooplankton biomass in temperate rivers. *Limnology and Oceanography* 41(7):1572-1577.

Billen G, Garnier J, Hanset P. 1994. Modeling phytoplankton development in whole drainage networks - the Riverstrahler model Applied to the Seine River system. *Hydrobiologia* 289(1-3):119-137.

Bradford ME, Peters RH. 1987. The relationship between chemically analyzed phosphorus fractions and bioavailable phosphorus. *Limnology and Oceanography* 32(5):1124-1137.

Bricker SB, Clement CG, Pirhalla DE, Orlando SP, Farrow DRG. 1999. National Estuarine Eutrophication Assessment: Effects of nutrient enrichment in the nation's estuaries. Silver Spring, Md.: U.S. Dept. of Commerce, National Oceanic and Atmospheric Administration.

CDWR [California Dept. of Water Resources]. 2004. California Irrigation Management Information System [accessed at <http://www.cimis.water.ca.gov>, 23 January 2004]. Sacramento, Calif.: California Dept. of Water Resources.

Cloern JE, Grenz C, Vidergar-Lucas L. 1995. An empirical model of the phytoplankton chlorophyll: Carbon ratio-the conversion factor between productivity and growth rate. *Limnology and Oceanography* 40:1313-1321.

Cloern JE. 2001. Our evolving conceptual model of the coastal eutrophication problem. *Marine Ecology Progress Series* 210:223-253.

Cole BE, Cloern JE. 1987. An empirical model for estimating phytoplankton productivity in estuaries. *Marine Ecology Progress Series* 36:299-305.

Conley DJ. 2000. Biogeochemical nutrient cycles and nutrient management strategies. *Hydrobiologia* 410:87-96.

CVRWQCB [Central Valley Regional Water Quality Control Board]. 1998. The water quality control plan (Basin Plan) for the California Regional Water Quality Control Board Central Valley Region. 4th ed. The Sacramento River Basin and the San Joaquin River Basin. Sacramento, Calif.: Central Valley Regional Water Quality Control Board.

CVRWQCB [Central Valley Regional Water Quality Control Board]. 2003. Total Maximum Daily Load for low dissolved oxygen in the San Joaquin River. Sacramento, Calif.: Central Valley Regional Water Quality Control Board.

Downing JA, McCauley E. 1992. The nitrogen:phosphorus relation in lakes. *Limnology and Oceanography* 37(5):936-945.

Ebbesmeyer CC, Cayan DR, McClain DR, Nichols FH, Peterson DH, Redmond KT. 1991. 1976 Step in the Pacific climate: Forty environmental changes between 1968-1975 and 1977-1984. In: Betancourt JL, Tharp VL, editors. *Proceedings of the Seventh Annual Climate (PACLIM)*

Workshop, April 1990. Interagency Ecological Study Program Technical Report 26. Sacramento, CA: California Department of Water Resources. p 115-126.

Efron B. 1983. Estimating the error rate of a prediction rule: improvements on cross-validation. *Journal of the American Statistical Association* 78:316-331.

Fisher TR, Melack JM, Grobbelaar JU, Howarth RW. 1995. Nutrient limitation of phytoplankton and eutrophication of inland, estuarine, and marine waters. In: Tiessen H, editor. *Phosphorus in the global environment*. Chichester: John Wiley & Sons. p 301-322.

Forsythe WC, Rykiel EJ, Jr., Stahl RS, Wu H, Schoolfield RM. 1995. A model comparison for daylength as a function of latitude and day of year. *Ecological Modelling* 80(1):87-95.

Gosselain V, Viroux L, Descy JP. 1998. Can a community of small-bodied grazers control phytoplankton in rivers? *Freshwater Biology* 39(1):9-24.

Gómez V, Maravall A. 2002. Seasonal adjustment and signal extraction in economic time series. Chapter 8. In: Pena D, Tiao GC, Tsay RS, editors. *A course in time series analysis*. New York: Wiley.

Harrell Jr. FE. 2001. *Regression modeling strategies: with applications to linear models, logistic regression, and survival analysis*. New York: Springer. 568 p.

Helsel DR, Hirsch RM. 1992. *Statistical methods in water resources*. New York: Elsevier.

IEP [Interagency Ecological Program]. 2003. Dayflow [accessed at <http://iep.water.ca.gov/dayflow>, 2 May 2003]. Sacramento, Calif.: Interagency Ecological Program for the San Francisco Estuary.

Jassby AD. 1999. Uncovering mechanisms of interannual variability in ecological time series. In: Scow K, Fogg G, Hinton D, Johnson M, editors. *Integrated assessment of ecosystem health*. Boca Raton, FL: CRC Press. p 285-306.

Jassby AD, Cloern JE, Cole BE. 2002. Annual primary production: patterns and mechanisms of change in a nutrient-rich tidal ecosystem. *Limnology and Oceanography* 47(3):698-712.

Jones & Stokes. 2002. City of Stockton Year 2001 sampling program. Data summary report for San Joaquin River Dissolved Oxygen TMDL. CALFED 2001 grant. Sacramento, Calif.: Jones & Stokes Associates.

Kilham SS, Kilham P. 1975. *Melosira granulata* (Ehr.) Ralfs: Morphology and ecology of a cosmopolitan freshwater diatom. Internationale Vereinigung für Theoretische und Angewandte Limnologie: Verhandlungen 19:2716-2721.

Kimmerer WJ. 2002. Effects of freshwater flow on abundance of estuarine organisms: physical effects or trophic linkages? Marine Ecology Progress Series 243:39-55.

Kiss KT. 1994. Trophic level and eutrophication of the River Danube in Hungary. Verhandlungen Internationale Vereinigung Limnologie 25:1688-1691.

Knowles N. 2002. Natural and human influences on freshwater inflows and salinity in the San Francisco Estuary at monthly to interannual scales. Water Resources Research 38(12):Art. No. 1289.

Knowles N, Cayan DR. 2002. Potential effects of global warming on the Sacramento/San Joaquin watershed and the San Francisco estuary. Geophysical Research Letters 29(18):Art. No. 1891.

Kratzer CR, Shelton JL. 1998. Water quality assessment of the San Joaquin-Tulare basins, California: Analysis of available data on nutrients and suspended sediment in surface water, 1972-1990. Professional Paper 1587. Denver, Colo.: U.S. Geological Survey.

Kratzer CR, Dileanis PD, Zamora C, Silva SR, Kendall C, Bergamaschi BA, Dahlgren RA. 2004. Sources and transport of nutrients, organic carbon, and chlorophyll-a in the San Joaquin river upstream of Vernalis, California, during summer and fall, 2000 and 2001. Water-Resources Investigations Report 03-4127. Sacramento, Calif.: U.S. Geological Survey.

Lam RHF, Brown JP, Fan AM, Milea A. 1994. Chemicals in California drinking-water - source contaminants, risk assessment, risk management, and regulatory standards. Journal of Hazardous Materials 39(2):173-192.

Leland HV, Brown LR, Mueller DK. 2001. Distribution of algae in the San Joaquin River, California, in relation to nutrient supply, salinity and other environmental factors. Freshwater Biology 46(9):1139-1167.

Lund JWG. 1964. Primary production and periodicity of phytoplankton. Verhandlungen Inter-

nationale Vereinigung Limnologie 15:37-56.

Morel A, Smith RC. 1974. Relation between total quanta and total energy for aquatic photosynthesis. *Limnology and Oceanography* 19(4):591-600.

Müller-Solger AB, Jassby AD, Müller-Navarra D. 2002. Nutritional quality of food resources for zooplankton (*Daphnia*) in a tidal freshwater system (Sacramento-San Joaquin River Delta, USA). *Limnology and Oceanography* 47(5):1468-1476.

Nichols FH. 1985. Increased benthic grazing: an alternative explanation for low phytoplankton biomass in northern San Francisco Bay during the 1976-1977 drought. *Estuarine, Coastal, and Shelf Science* 21:379-388.

OECD [Organization for Economic Cooperation and Development]. 1982. Eutrophication of waters. Monitoring, assessment, and control. Final Report. Paris: Organization for Economic Cooperation and Development, Environment Directorate, Cooperative Programme on Monitoring of Inland Waters (Eutrophication Control). 152 p.

Pace ML, Findlay SEG, Lints D. 1992. Zooplankton in advective environments - the Hudson River community and a comparative analysis. *Canadian Journal of Fisheries and Aquatic Sciences* 49(5):1060-1069.

Padisák J. 2004. Phytoplankton. In: O'Sullivan PE, Reynolds CS, editors. *The lakes handbook*. Volume 1. Limnology and limnetic ecology. Oxford: Blackwell Science. p 251-308.

Platt T, Sathyendranath S, Ravindran P. 1990. Primary production by phytoplankton - analytic solutions for daily rates per unit area of water surface. *Proceedings of the Royal Society of London, Series B* 241(1301):101-111.

Reynolds CR. 1997. *Vegetation processes in the pelagic*. Oldendorf/Luhe, Germany: Ecology Institute. 370 p.

Reynolds CS, Maberly SC. 2002. A simple method for approximating the supportive capacities and metabolic constraints in lakes and reservoirs. *Freshwater Biology* 47(6):1183-1188.

Sobczak WV, Cloern JE, Jassby AD, Müller-Solger AB. 2002. Bioavailability of organic matter in a highly disturbed estuary: The role of detrital and algal resources. *Proceedings of the National*

Academy of Sciences 99(12):8101-8105.

Stumm W, Morgan JJ. 1981. Aquatic chemistry. New York: Wiley-Interscience.

Trenberth KE, Hurrell JW. 1994. Decadal atmosphere-ocean variations in the Pacific. *Climate Dynamics* 9:303-319.

Wehr JD, Descy J-P. 1998. Use of phytoplankton in large river management. *Journal of Phycology* 34:741-749.

7 Tables

Table 1: Partial F tests for the Vernalis peak chlorophyll a model.

Factor	d.f.	Partial Sum Sq.	Mean Sq.	F -statistic	Prob.
Discharge	1	15	15	110	<0.001
Trend	2	2.4	1.2	9.0	<0.001
-nonlinearity	1	1.5	1.5	12	0.002
Regression	3	22	7.2	55	<0.001
Error	30	3.9	0.13		

Table 2: Coefficient values for the model describing net discharge (m^3/s) into the DWSC ($n = 71$).

Variable	Coefficient	Std. Error	t -Statistic	Prob.
Intercept	20	5	4.2	< 0.001
Q_{vern}	0.40	0.01	30	< 0.001
$Q_{xport}(1 - B_{hor})$	-0.081	0.019	-4.3	< 0.001

8 Figure Captions

1. Map of the San Joaquin Basin and River, including a portion of the Delta (modified from Figure 1 of Kratzer et al. 2004, with permission).

2. The San Joaquin River from Vernalis through the Stockton Deep Water Ship Channel. The locations of the Vernalis and Mossdale long-term monitoring stations are indicated, as well as the Wastewater Facility effluent (RWCF) and tidal velocity station (UVM). *Green line*, tidal portion of the river upstream of the Ship Channel. *Yellow line*, Ship Channel.
3. Monthly time series of chlorophyll *a* measurements and discharge estimates for the tidal San Joaquin River.
4. Principal component analysis of the chlorophyll *a* monthly time series. (A) Variance and cumulative variance corresponding to each principal component. *Shading*, statistically significant according to Rule N ($P < 0.05$). (B) Coefficients for the first principal component.
5. Estimated carrying capacities of available resources at Mossdale for phytoplankton, compared with actual chlorophyll *a* values. (A) Light carrying capacity. (B) Nitrogen and phosphorus carrying capacities.
6. (A) Molar ratio of total nitrogen to phosphorus at Vernalis. *Dashed line*, ratio = 16, characteristic of phytoplankton. (B) Long-term (Theil) trends by month for the molar ratio of total nitrogen to phosphorus at Vernalis, 1975–2002. *Shading*, significantly different from zero ($P < 0.05$), according to the Kendall-tau test.
7. Estimated phytoplankton community growth rates at Mossdale during the time of annual peak biomass, based on (1) and (7).
8. Annual chlorophyll peaks at Vernalis versus river discharge during the same month in which the peak occurred, 1969–2002. *Filled circles*, observations before 1978.
9. Partial residual plots for the Vernalis peak chlorophyll *a* model (11). (A) Partial residuals for discharge. (B) Partial residuals for the time trend. *Solid line*, partial fit. *Dashed line*, standard errors. *Circles*, partial residuals.

10. San Joaquin River discharge near Vernalis during July, including the water year type for each year. *C*, critical (critically dry). *D*, dry. *BN*, below normal. *AN*, above normal. *W*, wet.
11. July discharge as a proportion of total water year discharge for the Stanislaus River near its confluence with the San Joaquin River. *Dashed lines*, median values before and since 1980.
12. Total suspended solids versus discharge by month near Vernalis, 1969–2002. *Straight lines*, power relation between suspended matter and discharge, i.e., $M \propto Q_{vern}^a$.
13. Fitted values and actual observations of net discharge into the Ship Channel. Fitted values are based on the model described by (8).
14. Cause-and-effect diagram summarizing the linkages described in this study for regulation of peak annual phytoplankton biomass.

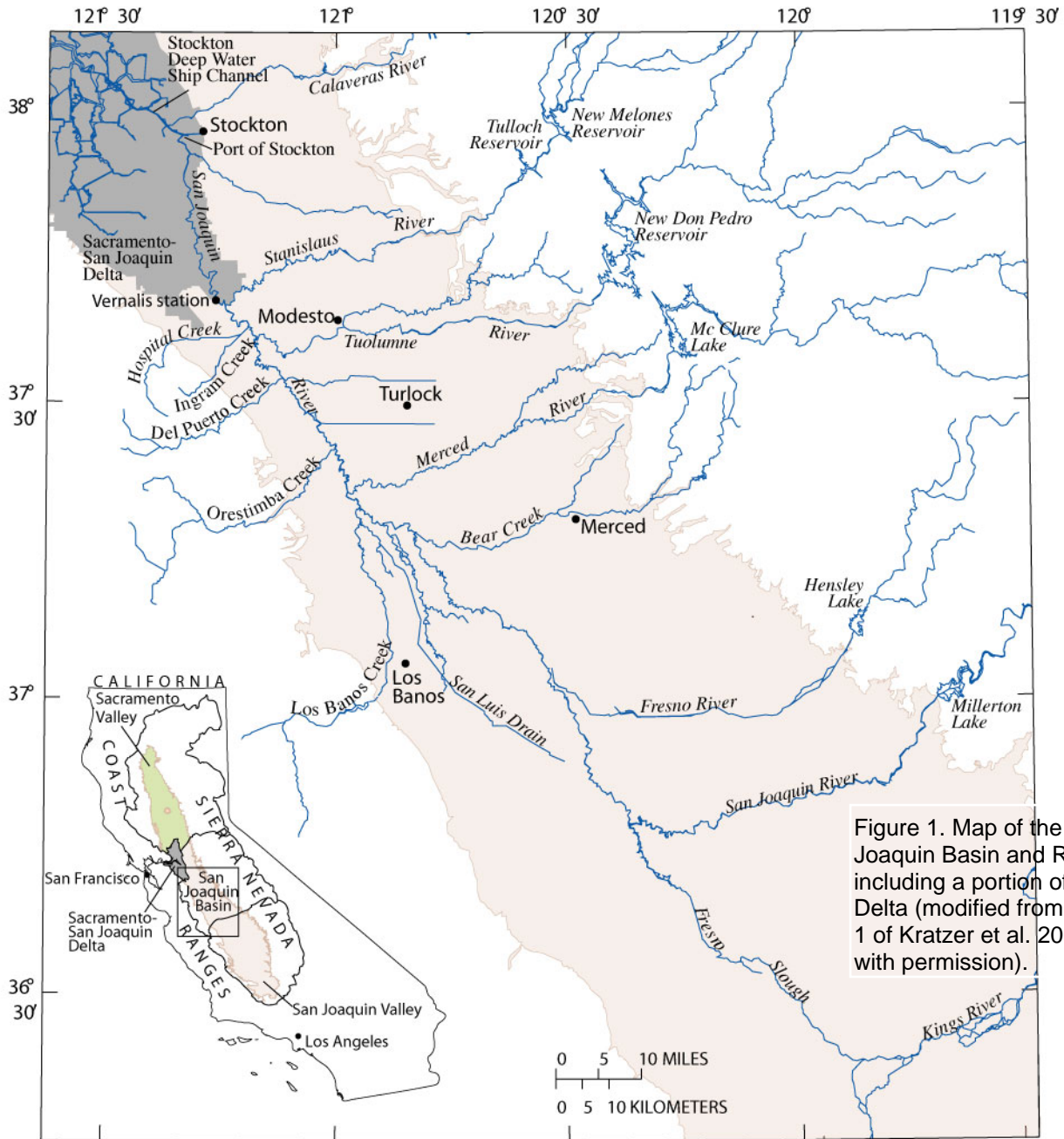


Figure 1. Map of the San Joaquin Basin and River, including a portion of the Delta (modified from Figure 1 of Kratzer et al. 2004, with permission).

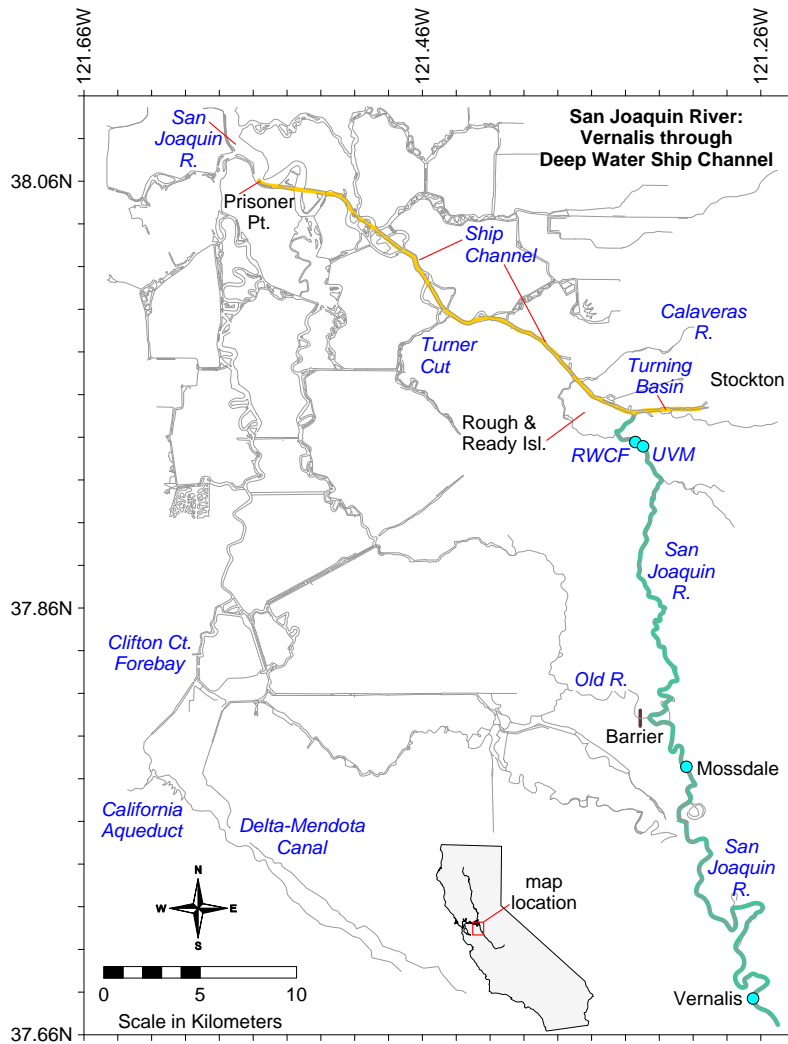


Figure 2: The San Joaquin River from Vernalis through the Stockton Deep Water Ship Channel. The locations of the Vernalis and Mossdale long-term monitoring stations are indicated, as well as the Wastewater Facility effluent (RWCF) and tidal velocity station (UVM). *Green line*, tidal portion of the river upstream of the Ship Channel. *Yellow line*, Ship Channel.

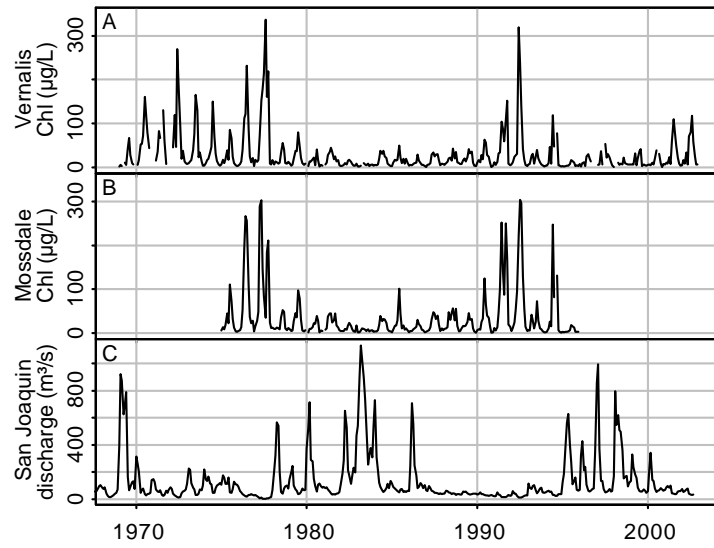


Figure 3: Monthly time series of chlorophyll *a* measurements and discharge estimates for the tidal San Joaquin River.

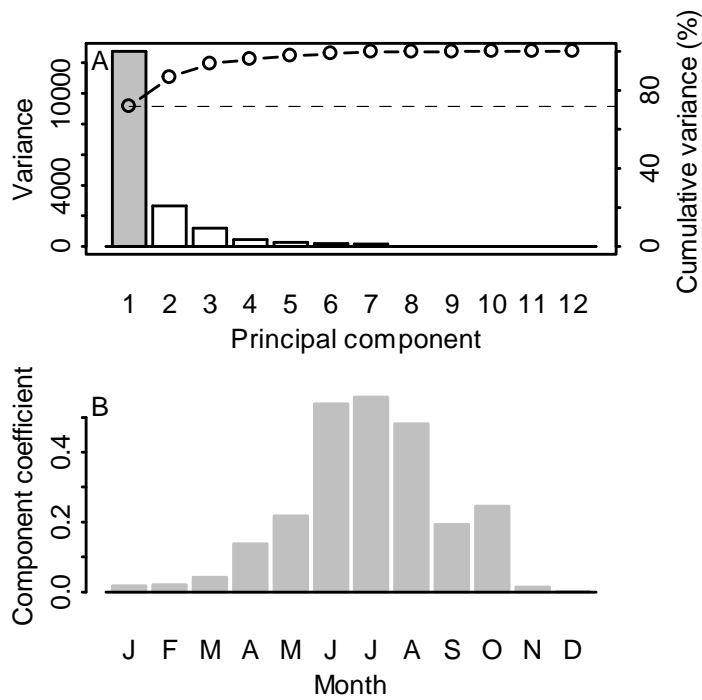


Figure 4: Principal component analysis of the chlorophyll *a* monthly time series. (A) Variance and cumulative variance corresponding to each principal component. *Shading*, statistically significant according to Rule N ($P < 0.05$). (B) Coefficients for the first principal component.

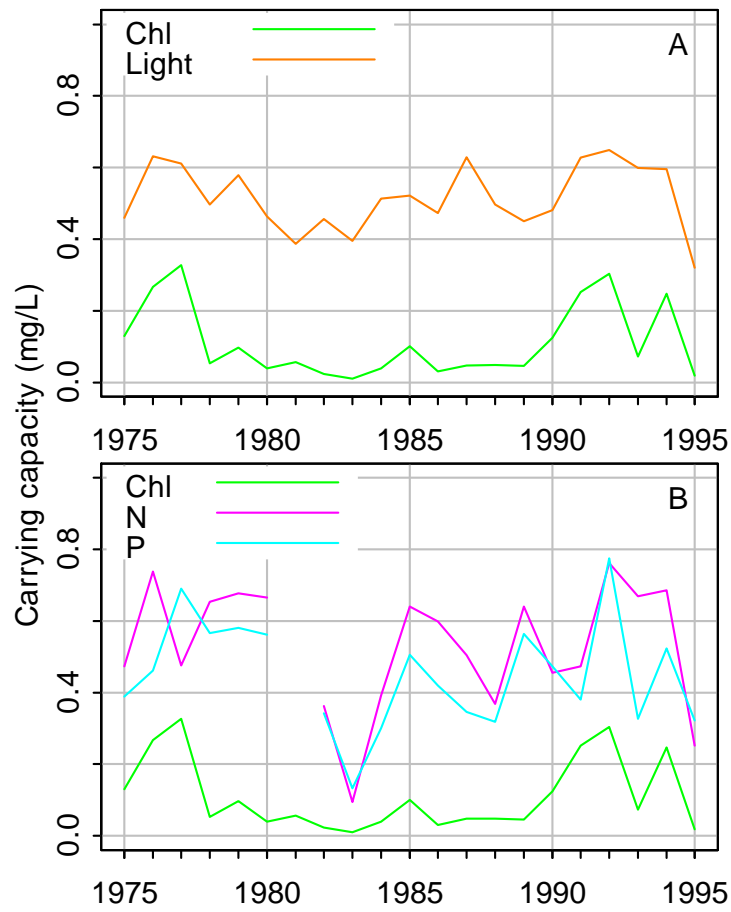


Figure 5: Estimated carrying capacities of available resources at Mosssdale for phytoplankton, compared with actual chlorophyll *a* values. (A) Light carrying capacity. (B) Nitrogen and phosphorus carrying capacities.

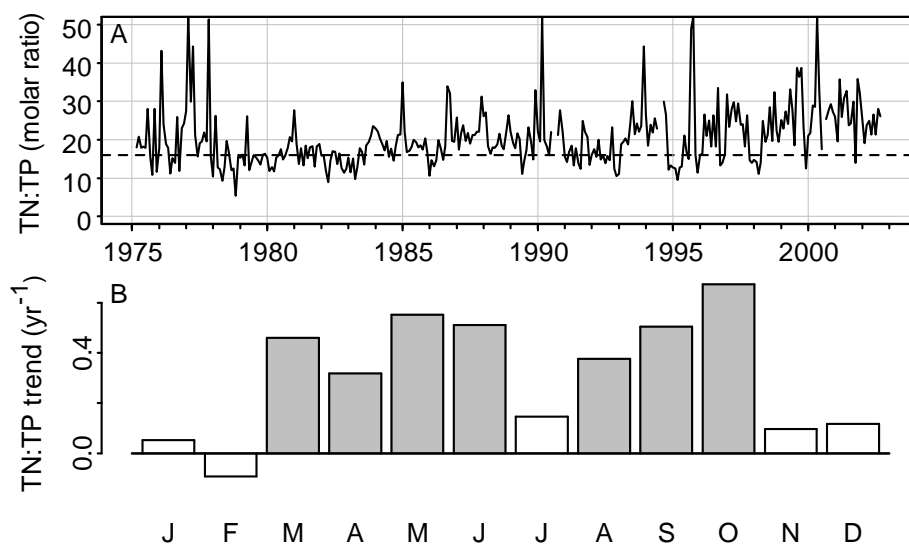


Figure 6: (A) Molar ratio of total nitrogen to phosphorus at Vernalis. *Dashed line*, ratio = 16, characteristic of phytoplankton. (B) Long-term (Theil) trends by month for the molar ratio of total nitrogen to phosphorus at Vernalis, 1975–2002. *Shading*, significantly different from zero ($P < 0.05$), according to the Kendall-tau test.

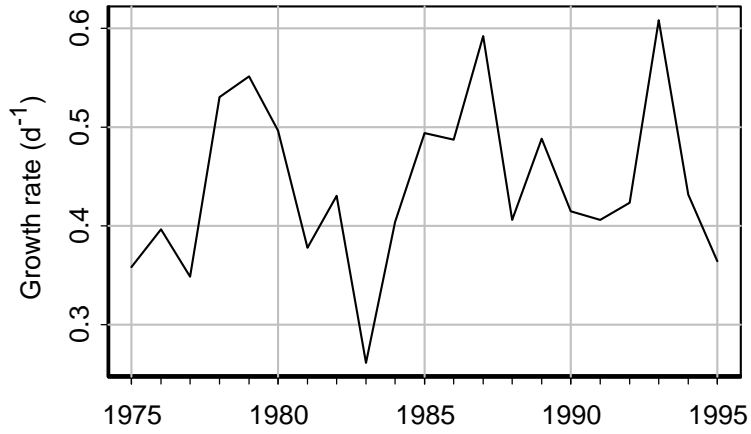


Figure 7: Estimated phytoplankton community growth rates at Mossdale during the time of annual peak biomass, based on (1) and (7).

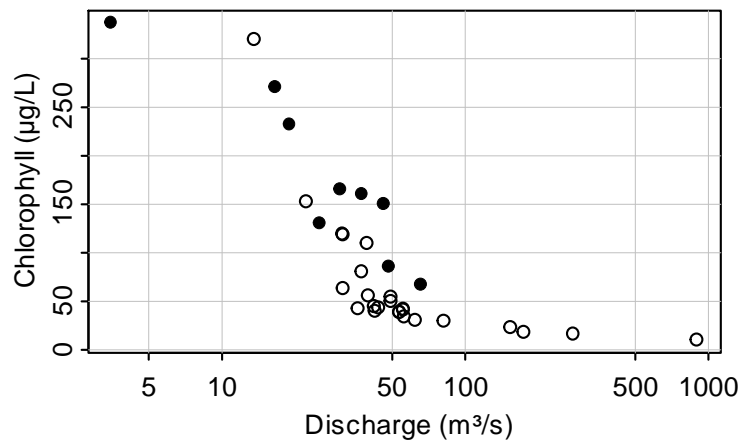


Figure 8: Annual chlorophyll peaks at Vernalis versus river discharge during the same month in which the peak occurred, 1969–2002. *Filled circles*, observations before 1978.

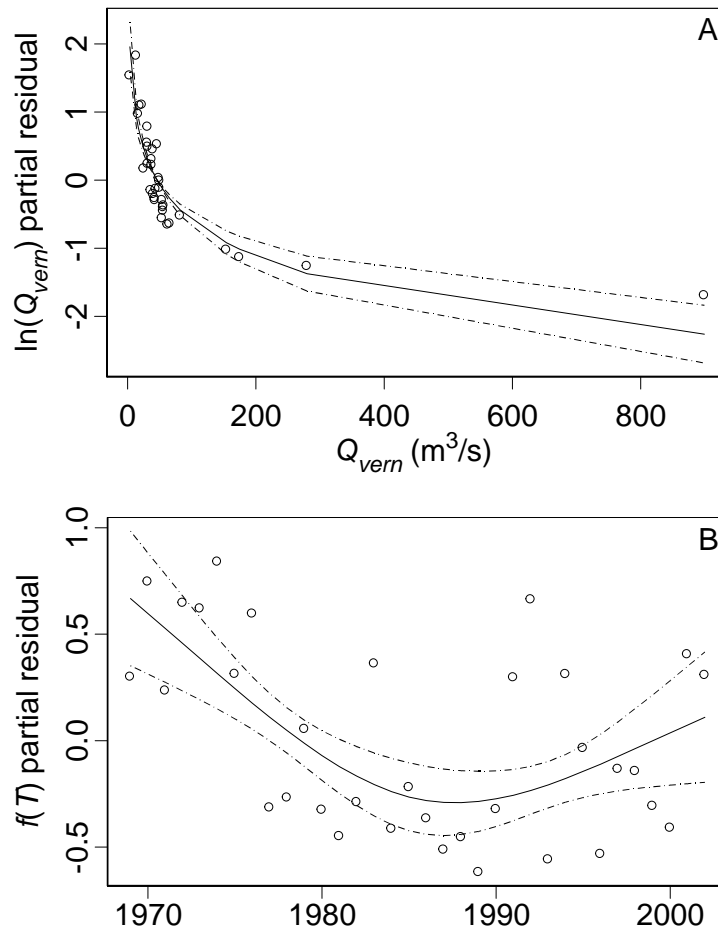


Figure 9: Partial residual plots for the Vernalis peak chlorophyll a model (11). (A) Partial residuals for discharge. (B) Partial residuals for the time trend. *Solid line*, partial fit. *Dashed line*, standard errors. *Circles*, partial residuals.

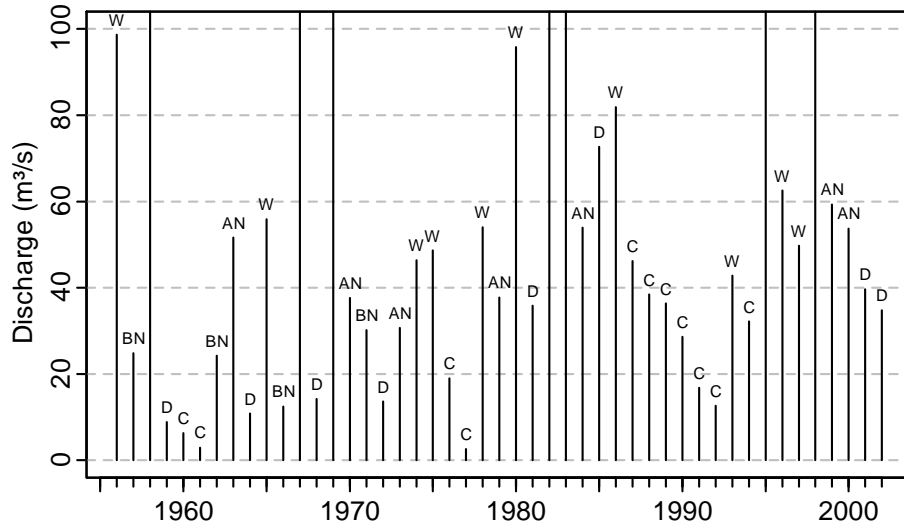


Figure 10: San Joaquin River discharge near Vernalis during July, including the water year type for each year. *C*, critical (critically dry). *D*, dry. *BN*, below normal. *AN*, above normal. *W*, wet.

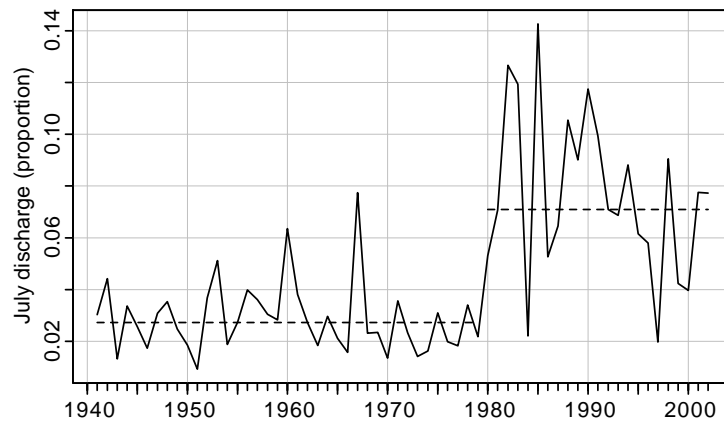


Figure 11: July discharge as a proportion of total water year discharge for the Stanislaus River near its confluence with the San Joaquin River. *Dashed lines*, median values before and since 1980.

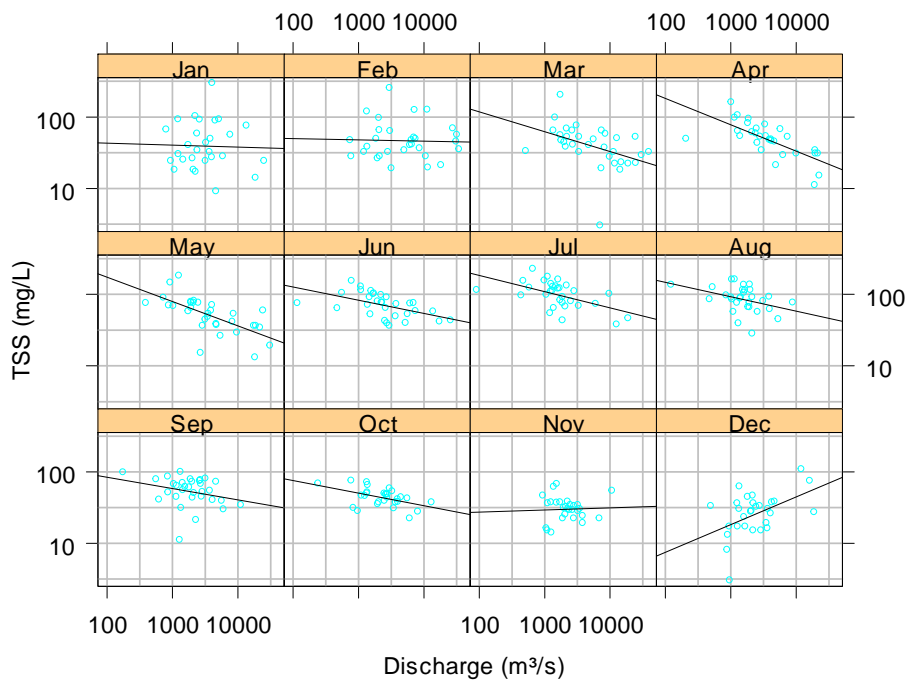


Figure 12: Total suspended solids versus discharge by month near Vernalis, 1969–2002. *Straight lines*, power relation between suspended matter and discharge, i.e., $M \propto Q_{vern}^a$.

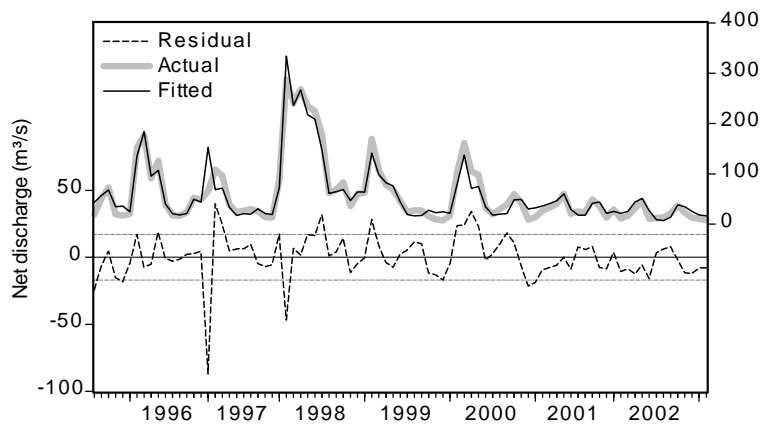


Figure 13: Fitted values and actual observations of net discharge into the Ship Channel. Fitted values are based on the model described by (8).

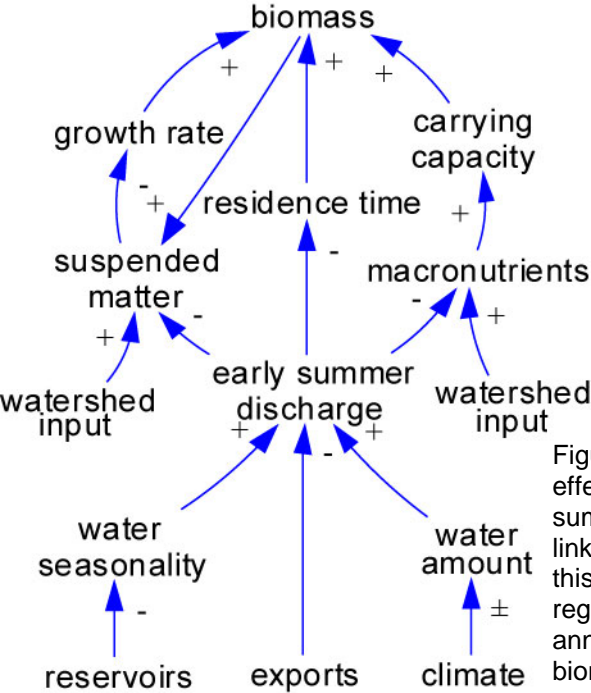


Fig
 effe
 sun
 link
 this
 reg
 an
 bio